Coseismic Deformation and a Fault Model for the Niigataken Chuetsu-oki Earthquake in 2007

Takuya NISHIMURA

Abstract

The Niigataken Chuetsu-oki earthquake in 2007 occurred just west of the coast of Kashiwazaki in Niigata Prefecture, central Japan on July 16, 2007. We present an overview of crustal deformation and fault models associated with the earthquake by reviewing three published papers by a group of the Geographical Survey Institute. The permanent GPS network (GEONET), interferometric analysis of SAR acquired by "Daichi" satellite (ALOS), and leveling clarify coseismic deformation in detail. Although it is difficult to determine which plane in two conjugate planes of the focal solution ruptured only from the geodetic data on land, a combination of a large southeast-dipping fault and a small northwest-dipping fault successfully explain the observed deformation and the aftershock distribution. The southeast-dipping fault is found to have released a seismic moment that is four times that released by the northwest-dipping conjugate fault. The interferograms reveal not only a large deformation near the source area of the earthquake but also a local uplift in the region of active folding, 15 km east of the earthquake epicenter. The 1.5-km-wide and 15-km-long band of uplift is located along the anticline axis of an active fold and cannot be explained by the elastic deformation resulting from the mainshock of the earthquake. This uplift suggests the episodic growth of active folds.

1. Introduction

A shallow earthquake occurred near the coast of Niigata Prefecture, Central Japan on July 16, 2007 (Fig. 1). The earthquake, with a JMA (Japan Meteorological Agency) magnitude of 6.8, was named the Niigataken Chuetsu-oki Earthquake in 2007 (hereafter, the 2007 Chuetsu-oki earthquake) by JMA. It caused around 2400 casualties, serious damage to buildings, liquefaction, and landslides near the epicenter, especially in Kashiwazaki. The focal mechanism from the Centroid Moment Tensor (CMT) inversion shows a thrust-type faulting with a compressional axis in the northwest-southeast direction (Fig. 1). The epicenter of the main-shock was under the Sea of Japan. Most aftershocks also occurred under the sea.

It is notable that the earthquake occurred in the Niigata-Kobe Tectonic Zone (NKTZ), where the geodetic strain rate is higher than the surrounding region. Sagiya et al. (2000) proposed NKTZ based on the spatial distribution of contemporary strain rate from a Japanese permanent GPS array, GEONET and the frequent occurrence of crustal earthquakes. One of the earthquakes is the M_{JMA} 6.8 2004 Chuetsu earthquake which occurred on October 23, 2004. Its epicenter was located only 40 km southeast of that of the 2007 Chuetsu-oki earthquake (Fig. 1).

There are several studies associated with the source mechanisms and crustal deformation of the Chuetsu-oki earthquake (e.g., Nishimura et al., 2008a; 2009; Kato et al., 2008, Ohta et al., 2008; Shinohara et al., 2008). The largest problem for the source mechanism was which nodal plane of the focal mechanism was ruptured by the earthquake. In other word, it was unclear whether the ruptured seismic fault dipped to the northwest or southeast. No geophysical measurements were conducted just above the source region of the earthquake because it occurred offshore. The spatial relation between the source and the observatory made it difficult for researchers to determine the source process and fault geometry of the 2007 Chuetsu-oki earthquake.

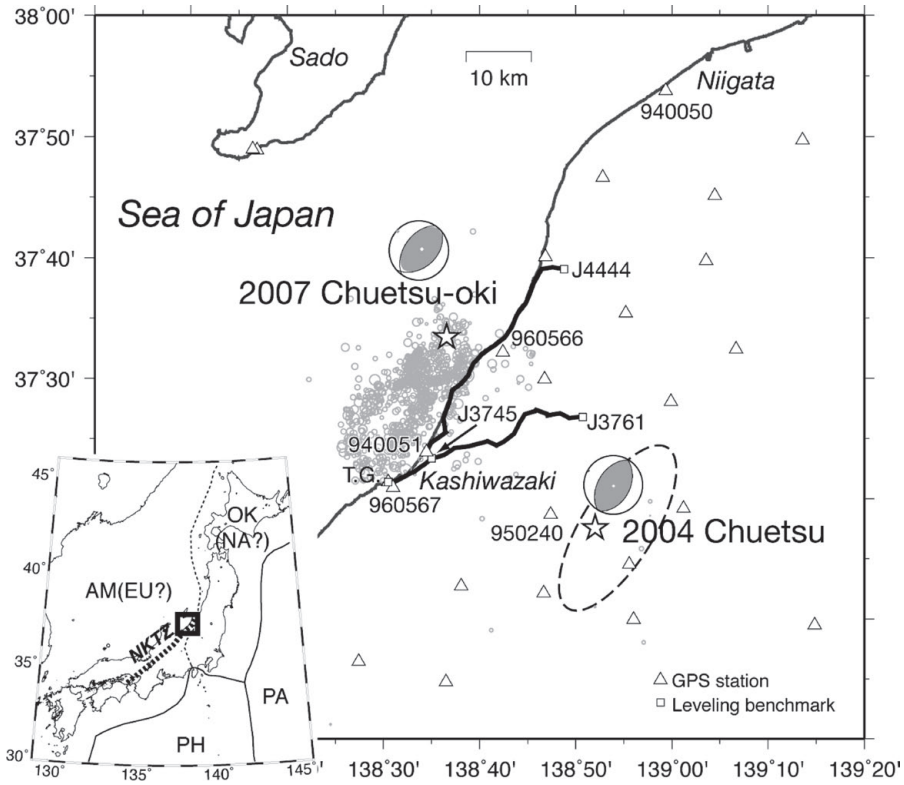

Fig. 1 Location map showing an epicenter of the 2007 Chuetsu-oki earthquake and geodetic stations (modified from Nishimura et al., 2008b). Open triangles represent the permanent GPS stations. Thick lines represent leveling routes with terminal and junction benchmarks denoted by open squares. Station codes of the selected GPS stations and leveling benchmarks are denoted. T. G. is the Kashiwazaki tide gauge station where leveling benchmarks and the permanent GPS stations locate. A star and gray circles represent epicenters of the mainshock and aftershocks of the 2007 Chuetsu-oki earthquake, respectively. The epicenter of the 2004 Chuetsu earthquake is also shown by a star. Beach balls represent CMT solution for the focal mechanism determined by NIED (National Research Institute for Earth Science and Disaster Prevention). Abbreviations in tectonic map (inset) are OK, NA, PA, PH, EU, AM, and NKTZ for the Okhotsk, North American, Pacific, Philippine Sea, Eurasia, Amurian plates, and Niigata Kobe Tectonic Zone respectively.

It was difficult to determine the fault geometry purely from the hypocenters determined from data from a permanent seismometer network (e.g., JMA catalog) because the aftershock distribution showed both northwest- and southeast-dipping complex alignments. Shinohara et al. (2008) started the temporal seismic observation using pop-up type Ocean Bottom Seismometers (OBSs) to relocate the hypocenter of the aftershocks accurately. The relocated distribution shows that in the entire aftershock region, most aftershocks occurred along a southeast-dipping plane. They therefore concluded that the major fault ruptured by the mainshock dipped to the southeast. Nishimura et al. (2009) proposed that both a southeast-dipping fault and a small northwest-dipping fault were ruptured by the earthquake based on the geodetic data and the aftershocks relocated by Shinohara et al. (2008). Kato et al. (2008) also reached a similar conclusion from the distribution of aftershocks just after the mainshock.

In this paper, we overview crustal deformation and fault models related to the 2007 Chuetsu-oki earthquake based on a review on the papers by a group of the Geographical Survey Institute (GSI) (Nishimura et al., 2008a, 2008b, 2009). We also present a kinematic analysis of 1-sec sampling GPS data for the earthquake.

2. Geodetic Data

2.1 GPS

Significant coseismic deformation associated with the 2007 Chuetsu-oki earthquake was observed at GEONET stations in central Japan. The Japanese islands are covered by a permanent GPS array, GEONET, which

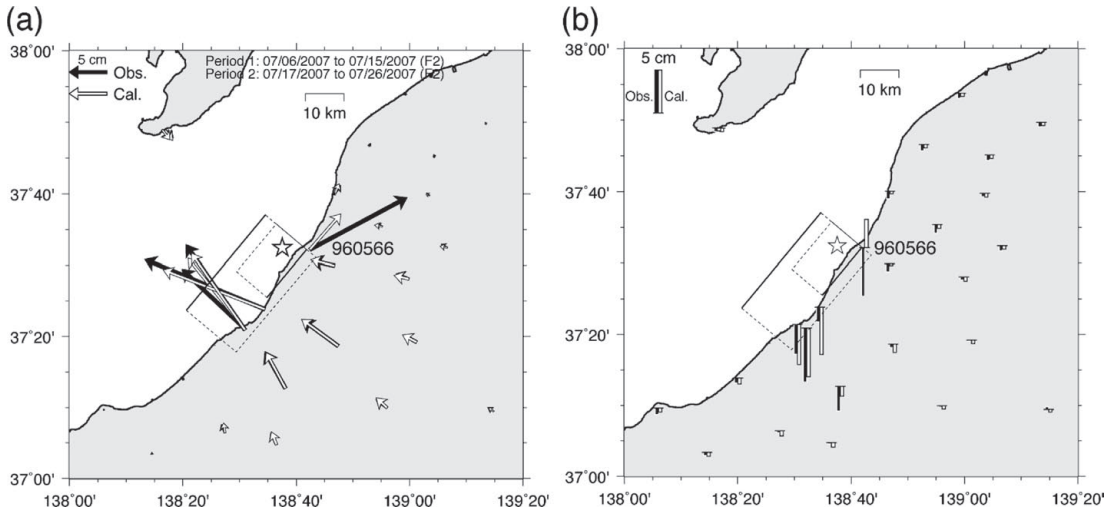

Fig. 2 Coseismic displacement of the 2007 Chuetsu-oki earthquake at permanent GPS stations (Nishimura et al., 2009). A star represents an epicenter of the main-shock relocated by Shinohara et al. (2008). The plotted displacement is relative to Toyama (950249) station. The dotted rectangles show the fault model (Nishimura et al., 2009). The solid line on the rectangles shows the upper edge of the fault. (a) Horizontal displacement. Solid and open arrows represent observed and calculated displacements, respectively. (b) Vertical displacement. Solid and open bars represent observed and calculated displacements, respectively.

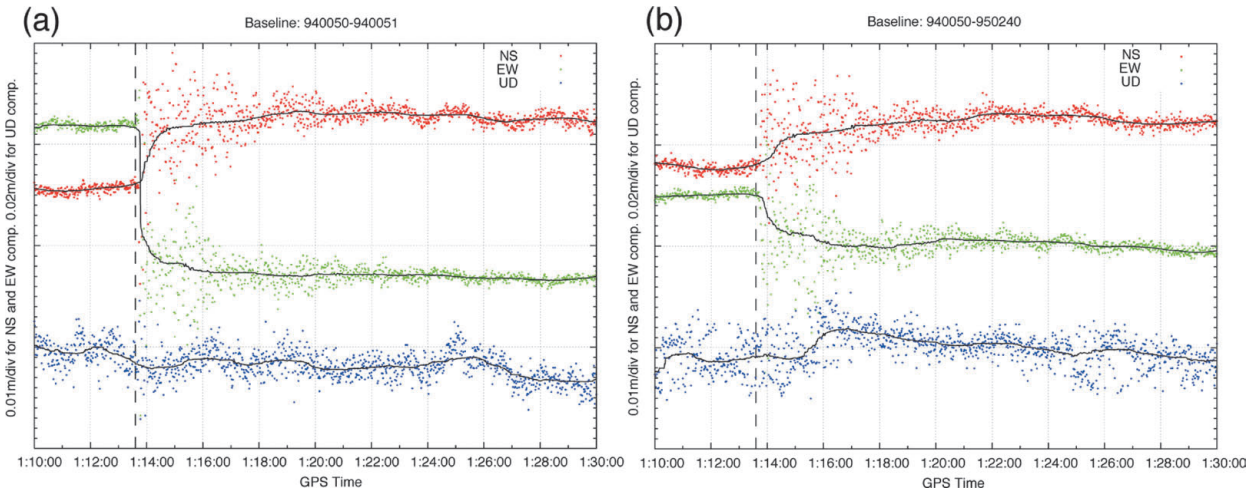

Fig. 3 Time-series of relative coordinates of GPS stations with 1-second sampling. Horizontal axis is GPS time (= JST - 9 hours – 14 seconds) as of July 16, 2007. Solid curves represent running median for 121 seconds. Dashed vertical lines represent the occurrence of the 2007 Chuetsu-oki earthquake. (a) 940051(Kashiwazaki1) relative to 940050(Niigata). (b) 950240(Ojiya) relative to 940050(Niigata).

consists of about 1240 continuous sites (see, e.g., Sagiya et al., 2000). Figs. 2a and 2b show the coseismic displacement in horizontal and vertical components, respectively. The maximum horizontal displacement is around 170 mm to the west-northwest at 940051 station. Subsidence is significant at several stations south of the epicenter. The plotted coseismic displacement is the difference in the average positions of daily solutions between July 6-15 and July 17-26, 2007. The spatial pattern of the coseismic displacement suggests compression in the northwest-southeast direction, which is concordant with the focal mechanism shown in Fig. 1.

Onsite measurements by GSI's staff and postseismic GPS measurements (Ohta et al., 2008) suggest that the large displacement observed at 960566 just east of the epicenter, was contaminated by local disturbance and monument instability. Tiltmeters in the monument and onsite measurements confirm that the

GPS pillar of 960567 was also tilted by strong ground shaking. The displacement plotted in Fig. 2 is corrected for pillar tilting by subtracting the antenna displacement relative to the base.

Significant postseismic displacement was recognized to reach around 20 mm for several months after the earthquake at 940051 station (GSI, 2008). The postseismic deformation is also observed at temporal GPS stations set up by a group of universities (Ohta et al., 2008).

Most of the GEONET stations have a capability of 1-second sampling and real-time data transmission to the analysis center in the headquarters of GSI (Yamagiwa et al., 2006). We estimate relative coordinates of the GEONET station data with 1-second sampling using the post-process kinematic analysis. The analysis software is RTD based on Epoch-by-Epoch^{TM} algorithm developed by Geodetics Inc. Fig. 3 shows a time-series including the earthquake. It clearly shows coseismic offsets and strong shaking of the ground. Scattered coordinates continued for more than 6 minutes after the earthquake. This seems to be caused by long-lasting surface waves in a region of thick sediment because the reference station is 940050 (Niigata) in the Echigo alluvial plain. The solid curves in Fig. 3 are filtered time-series by calculating moving the median for 121 seconds. Even in the strong shaking by surface waves, it is possible to detect the coseismic offset from the filtered time-series for several minutes after the earthquake. It should be expected to realize it in real-time because a loose constraint (i.e., 0.5 m) of prior coordinates of the GPS stations was used in the baseline analysis. If a tight constraint (i.e., 0.2 m) is used in the baseline analysis, the repeatability of the estimated time-series is so small that we can get a good result for the case of the Chuetsu-oki earthquake. However, it is not practical to use a tight constraint in a real time analysis because we do not know how large coseismic displacements will occur in future earthquakes. The coseismic displacement calculated from the kinematic analysis is equal to that from static analysis of the GEONET routine analysis in horizontal components within 2 cm. It confirms the feasibility of a real-time kinematic analysis of GPS to detect coseismic displacement immediately after large earthquakes. Crustal deformation research division in GSI now develops a method to estimate a fault model of the earthquake using a real-time GPS analysis.

2.2 InSAR

The L-band SAR data acquired by the Advanced Land Observation Satellite (ALOS), also called "Daichi," were used to map the spatial distribution of coseismic and postseismic deformation of the 2007 Chuetsu-oki earthquake (Nishimura et al., 2008a; 2008b). The SAR data obtained on different days in both descending and ascending orbits have been processed in order to generate interferograms (Fig. 4). The coherence of the interferograms is excellent, except in the coastal sand-dune region where considerable soil liquefaction and lateral soil flow were observed in field investigations after the earthquake. The SAR interferograms show the range change between the ground and the satellite, that is, the line-of-sight (LOS) displacement. Because the direction of the LOS is different for the descending and ascending orbits, the patterns of the fringes in the interferograms differ for the two orbits. The unitary vectors along the LOS in the descending and ascending orbits are (0.637, –0.113, 0.762) and (–0.620, –0.109, 0.777), respectively, in the coordinate set (east, north, up). The interferograms for the period including the earthquake (Figs. 4a, 4b, 4c, and 4f) clearly show coseismic deformation. A large displacement of around 300 mm was recognized south of the epicenter in the interferogram for the descending orbit (Fig. 4f). In contrast, the maximum displacement is around 150 mm in that for the ascending orbit (Figs. 4a, 4b, and 4c). In these interferograms, two peaks of the LOS displacement are found to be located in an area to the north of Kashiwazaki basin and the western part of the Nishiyama hills. Nishimura et al. (2008a, 2009) used interferograms for both the descending and ascending orbits (Figs. 4a and 4f) to estimate the fault model of the Chuetsu-oki earthquake.

2.3 Leveling

The 2007 Chuetsu-oki earthquake occurred near the first-order leveling route conducted by GSI (Fig. 1). One of the leveling routes is located along the coast (hereafter route A). The other goes from J3745 in Kashiwazaki to the inland (hereafter route B). These routes were leveled from September to October 2006, before the earthquake. GSI sent a survey team to re-level these routes just after the earthquake. The first period of the postseismic measurement was from July 20 to August 9, 2007. Most of route A except the northernmost part (i.e., from T. G. to 4451) and the west part of the route B (i.e., from J3745 to 3749) were leveled for this period. Another postseismic measurement was conducted for the

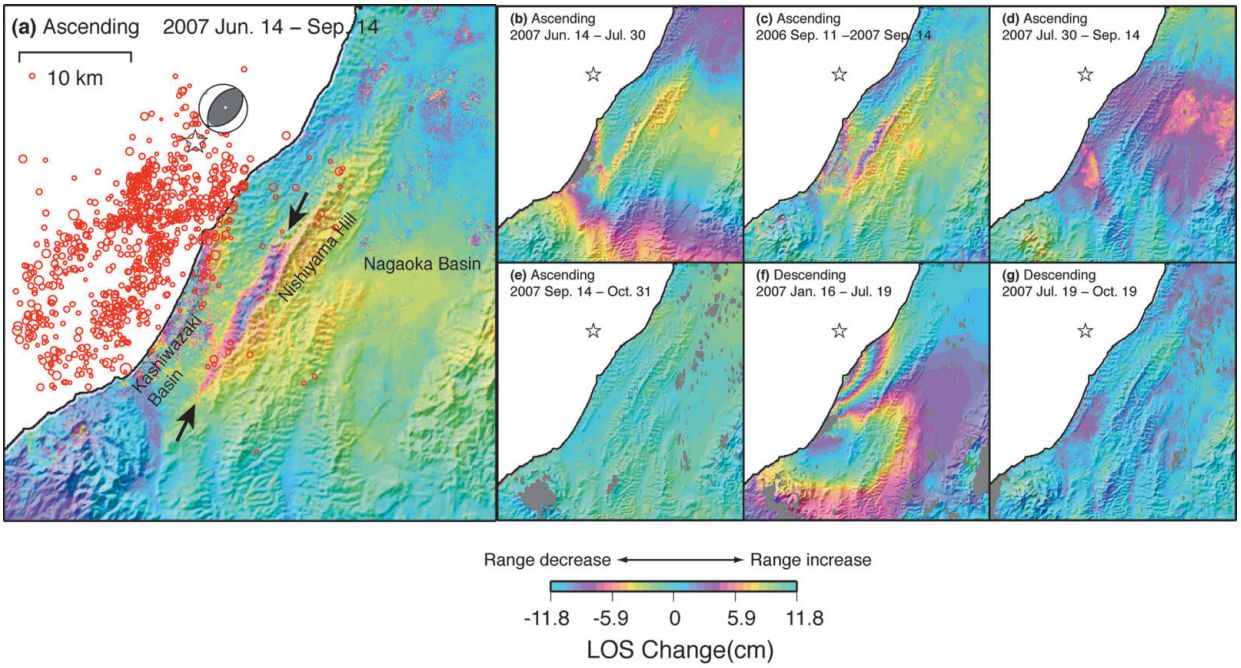

Fig. 4 Synthetic aperture radar interferograms acquired by "Daichi" satellite (Modified from Nishimura et al., 2008a). The image is superposed on the top of shaded topography. (a) Image is generated from data acquired from ascending orbit on June 14 and September 14, 2007. It clearly shows the belt-like uplift on the west side of the Nishiyama hills, indicated by the two black arrows. The star and red circles represent the epicenters of the mainshock and aftershocks of the Chuetsu-oki earthquake determined by JMA, respectively. Images generated from data acquired from ascending orbit on (b) June 14 and July 30, 2007; (c) September 11, 2006 and September 14, 2007; (d) July 30 and September 14, 2007; (e) September 14 and October 31, 2007. (f) Image generated form data acquired from descending orbit on January 16 and July 19, 2007; (g) September 14 and October 31, 2007.

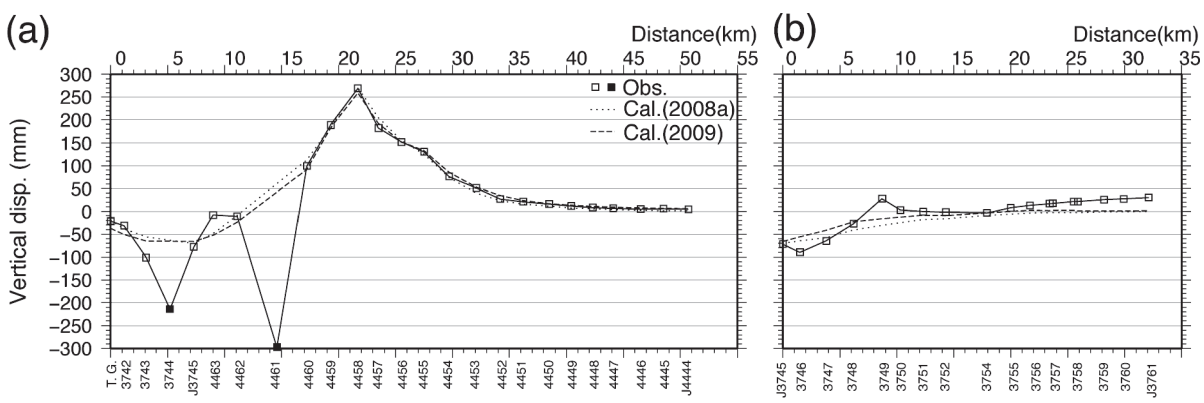

Fig. 5 Vertical displacement measured by leveling. Squares and circles indicate observed and calculated displacement (Nishimura et al., 2008a; 2009), respectively. Data indicated by solid squares may be affected by local disturbances and have not been used in the analysis of the fault model. Numbers at the bottom represent benchmark codes.

period from September 21 to October 4, 2007. The northernmost and southern part of route A (i.e., from 4451 to J4444 and from T. G. to J3745) and all of route B were leveled for the period. We used the data for the first period if the benchmarks have been leveled twice after the earthquake.

The vertical displacement observed by leveling surveys is roughly characterized by the uplift near the northern part of the aftershock area and the subsidence near its southern part (Fig. 5). The displacement in Fig. 5 is not absolute but a relative one for plotting. The maximum uplift of 264 mm with respect to J4444 is observed at 4458 near the northern part of the aftershock area. The maximum subsidence is 302 mm at 4461 with respect to J4444. Large troughs at 4461 and 3744 may be caused by local effects such as soil liquefaction and lateral soil flow because they are located in an incoherent part of the SAR interferograms (Figs. 4a, 4b, 4c and 4f). The benchmark at the Kashiwazaki tide gauge station abbreviated by T. G. subsided by 26 mm with respect to J4444. The subsidence of T. G. measured by continuous GPS and sea level are 35 mm and around 35 mm, respectively. Measurements by three different methods confirm subsidence of T. G. within around 10 mm uncertainties.

3. Coseismic fault model

Nishimura et al. (2008b, 2009) estimated the source model using the geodetic data. Nishimura et al. (2008b) constructed a preliminary fault model by inverting the observed deformation. The model assumes simple rectangular faults and homogeneous elastic half-space. They first tried to explain the observed displacement by a single rectangular fault. However, it was impossible to fit the displacement observed by GPS and InSAR especially near the aftershock region. Their model, therefore, consists of two rectangular faults whose moment magnitude is 6.7 in total (Fig. 6). The northeastern and southwestern segments dip northwest and southeast, respectively.

There are two problems in the fault model of Nishimura et al. (2008b). The first problem is a significant difference between aftershock distribution and the geodetic model in a depth of the source area. At the time of the estimation of Nishimura et al. (2008b), available aftershock distribution was limited to one determined without OBSs. Because the sediment layer in and around the epicentral area is extremely thick, with a thickness greater than 5 km, depths of aftershocks were overestimated in most analyses. On the other hand, a low-elastic modulus layer such as a sediment layer causes the half-space equivalent dislocation to appear shallower than the actual dislocation in the layered half

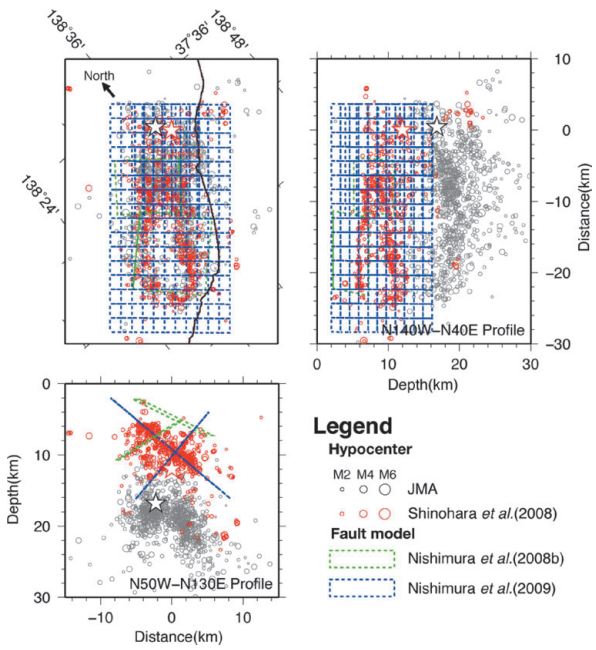

Fig. 6 Aftershock distribution and geometry of fault models of Nishimura et al. (2008b, 2009). Red and Black stars represent hypocenter of the mainshock determined by JMA and Shinohara et al. (2008), respectively.

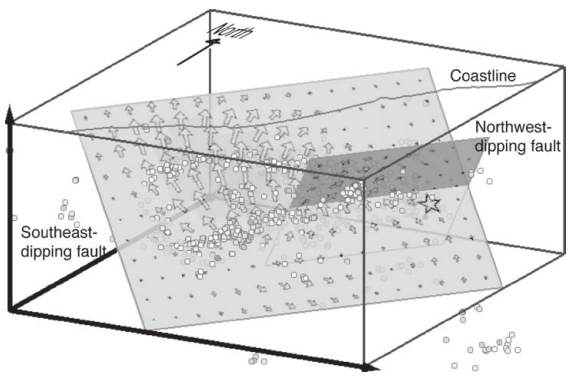

Fig. 7 Three-dimensional view of the slip distribution of the Chuetsu-oki earthquake and the aftershock distribution relocated by Shinohara et al. (2008) (Nishimura et al., 2009).

space for the modeling of crustal deformation (Savage, 1998). It was therefore necessary to use the same structure of seismic velocity and elastic modules in estimation of fault model and hypocenter relocation.

Another problem is whether the ruptured seismic fault dips to the northwest or southeast. It was difficult to determine the fault geometry purely from the hypocenters in JMA catalog because the aftershock distribution shows both northwest- and southeast-dipping complex alignments in the depth range of 14–28 km (Fig. 5). Nishimura et al. (2008b) mentioned the difficulty of determining the fault dip purely from geodetic data. However, the precise relocation of the aftershock using the data of OBSs (Shinohara et al., 2008) gave a casting vote to choose one of the nodal planes. The relocated distribution shows that in the entire aftershock region, most aftershocks occurred in the depth range of 6–15 km along a southeast-dipping plane. It provides strong evidence of the major fault ruptured by the mainshock dipping to the southeast.

Nishimura et al. (2009) proposed the fault model to solve these problems. They assumed that the fault followed the aftershock alignment relocated by Shinohara et al. (2008). The upper edge of the main southeast-dipping fault was 2 km deep, while the length and width of the fault were 32 and 22 km, respectively. The strike and dip of the fault were 220º and 40º for the southeast-dipping fault. They also assumed a small fault plane that is 16 km long and 14 km wide only in the northeastern part of the aftershock area. Its upper edge is located 4 km deep. The strike and dip of the northwest-dipping fault are 40º and 50º, respectively. They used a Green's function approach involving a multilayered medium to calculate the surface displacement due to dislocation sources (Wang et al., 2003). They then inverted the geodetic data to estimate slip distribution on the faults. The maximum slip on the southeast-dipping fault is 1.75 m in the southwestern part of the fault. The depth of the main slip ranges from 3 to 12 km. The slip on the northwest-dipping fault is of the reverse type and is a part of the right-lateral strike slip; it has a peak slip of 1.19 m in the southwestern part of the fault. The seismic moment released on the northwest-dipping fault is one-fourth of that released on the southeast-dipping fault. Comparing the slip distribution of the fault model and the aftershock

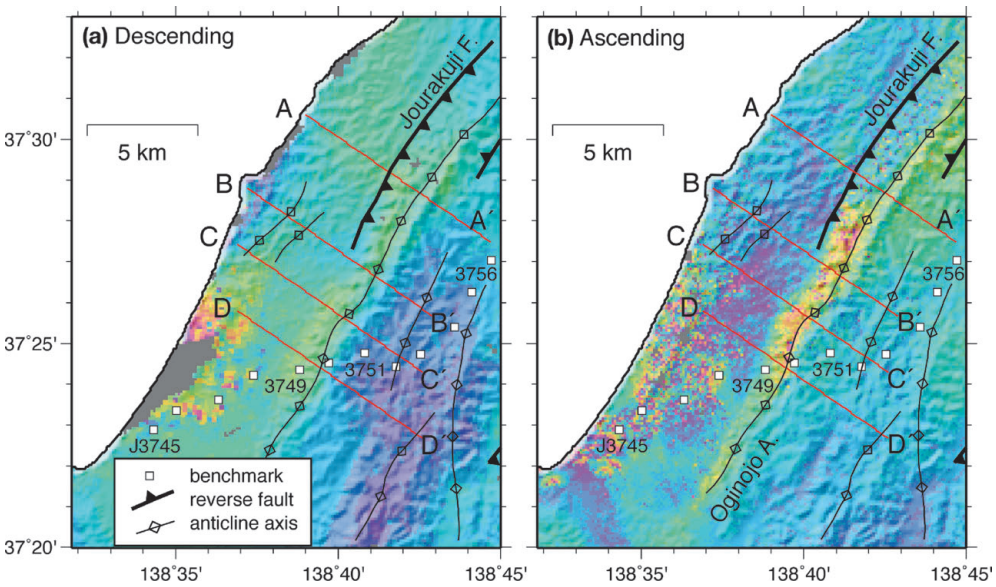

Fig. 8 Residual LOS displacement in and around the Nishiyama hills (Nishimura et al., 2008a). The coseismic deformation predicted by the fault model of Nishimura et al. (2009) is removed from the original InSAR images shown in Fig. 4. Active fault traces (Research Group for Active Faults of Japan, 1991), anticline axes (Kobayashi et al., 1995) and leveling benchmarks are also plotted. The four lines indicate the lines of profiles used for plotting two-dimensional displacement. (a) Images from (a) descending orbit data (Fig. 4f shows original interferogram) and (b) ascending orbit data (Fig. 4a shows original interferogram).

distribution (Fig. 7), it is clear that many aftershocks occurred near the deep edge of the large-slip area on the southeast-dipping fault. The relation between the two distributions can be interpreted as follows: many aftershocks occur in the area where the coseismic slip of the mainshock increased the stress. The largest slip occurs in the gap of aftershocks in the southwestern part of the fault. This supplementary relation between the coseismic slip and aftershocks has been observed during many earthquakes (e.g., Yagi et al., 1999). Nishimura et al. (2009) mentioned that only the southeast-dipping fault could explain the observed deformation. However the model of the only southeast-dipping fault shows spatial roughness in slip distribution and no clear relation between the slip and aftershocks. From these reasons, it is reasonable that the main fault ruptured by the 2007 Chuetsu-oki earthquake dips to the southeast with the minor northwest-dipping fault only in the northeastern part of the aftershock region.

4. Episodic growth of active fold

Nishimura et al. (2008a) analyzed the SAR interferograms in detail. The SAR interferograms clearly show not only large deformation along the coastline but also a narrow deformation band in the Nishiyama hills (Fig. 4). The deformation zone in the interferograms for the ascending orbit (Figs. 4a, 4b, and 4c) is a narrow band extending along the NNE-SSW direction and is approximately 1.5-km wide and 15-km long. A small offset of fringes can be observed in the Nishiyama hills, even in the interferogram for the descending orbit (Fig. 4f). The signal observed in the Nishiyama hills cannot be an artifact of the InSAR processing. A possible major source of error in the InSAR analysis is an error in the digital elevation model (DEM) used to remove topographic fringes. However, a DEM error is precluded because the DEMs provided by the Geographical Survey Institute (GSI) and Shuttle Radar Topography Mission (SRTM) have produced almost the same fringe patterns. The other possible major source of error is heterogeneity in the delay of radio waves in the atmosphere and ionosphere. Although the fringes caused by these effects tend to change rapidly with time, the narrow band of the fringes in the Nishiyama hills is clear in all coseismic interferograms (Figs. 4a, 4b, and 4c). Nishimura et al. (2008a) therefore concluded that the narrow band of fringes represents actual ground deformation.

After subtracting the range change predicted by the fault model of Nishimura et al. (2009) from the observed interferograms, a narrow band of a smaller range remains. The overlaying tectonic structures on the residual interferograms (Fig. 8) show that the Oginojo anticline is parallel to this band and is at the eastern rim of the band. The Jourakuji fault, an east-dipping active fault, borders the western rim of the northern part of the deformation band. Combining the interferograms for the descending and ascending orbits (Fujiwara et al., 2000), we obtain the displacement in quasi-upward (elevation angle is 82º from the south) and eastward directions (Fig. 9). The displacement vectors along four profiles across the deformation band show that the uplift and westward displacement are bounded by the Oginojo anticline and the southern extension of the Jourakuji fault. The vectors in the surrounding region show compressional deformation. The spatial coincidence of the uplift band and Oginojo anticline suggest the growth of active folds. Leveling data also show an uplift at benchmark 3749

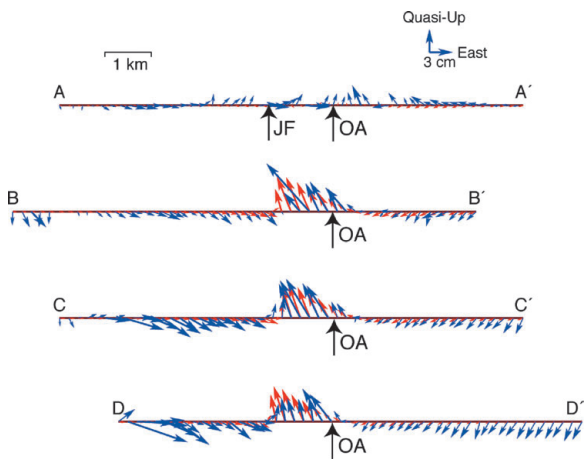

Fig. 9 Two-dimensional displacement vectors along profiles AA´ to DD´ shown in Fig. 8 (Nishimura et al., 2008a). The blue and red vectors show the displacements obtained from the residual interferograms and calculated using the fault model. OA and JF indicate the locations of the Oginojo anticline and Jourakuji fault, respectively. The four profiles are shifted to center the location of the Oginojo anticline.

(Fig. 5b) in the Nishiyama hills, which confirmed the InSAR analysis. According to Koarai et al. (2009), no significant deformations implying the growth of active folds were recognized by a field observation in and around the deformation zone.

The displacement vectors (Fig. 9) can be interpreted in terms of the east-dipping reverse fault under the uplift band. The data from the residual interferograms and residual vertical displacement of leveling were therefore inverted to estimate the parameters of a rectangular fault in an elastic half-space. The result (Nishimura et al., 2008a) indicates the presence of a slip on the east-dipping reverse fault just beneath the uplift band, which can be interpreted as aseismic slip on the southern extension of the Jourakuji fault. The rectangular fault is 9.9 ± 0.8 km long and 1.8 ± 0.1 km wide with a strike of 31º ± 1º and a dip of 41º ± 3º. The fault slips by 100 ± 12 mm with a rake of 93 ± 8º. The depth of the fault ranges from 0.1 ± 0.1 to 1.3 ± 0.2 km. The uncertainties in the parameters are introduced by formal errors (1 sigma) of the inversion. Assuming a rigidity of 1.3 GPa, the moment magnitude is found to be 4.2. This fault model provides a logical explanation of the observed data (Fig. 9).

The uplift upon the occurrence of the Chuetsu-oki earthquake can be regarded as an episodic slip event on the existing shallow reverse fault. Nishimura et al. (2008a) proposed two possible causes of the episodic acceleration. One cause is the static stress triggering by the mainshock of the Chuetsu-oki earthquake. This is supported by the calculation of the Coulomb stress change using the coseismic fault model. The other possible cause involves the fault geometry of the Chuetsu-oki earthquake. As explained in Sec. 3, a minor fault dipping to the northwest was ruptured in the northern part of the aftershock area. If such a fault extends into the shallow sedimental layer and terminates below the uplift band, the stress on the shallow reverse fault effectively increases.

5. Concluding remarks

The crustal deformation associated with the 2007 Chuetsu-oki earthquake is clarified by the measurements and investigation conducted by GSI. The geodetic measurement including GPS, InSAR, and leveling contributed to understanding the mechanism of the earthquake. However, the earthquake reminded us of the non-uniqueness of the estimated fault model from the geodetic data without the data just above the source fault. Even though the InSAR data provided distribution of the coseismic deformation, a combination with the precise aftershock distribution was necessary to estimate a plausible slip distribution on major southeast-dipping and minor northwest-dipping faults.

On the other hand, the InSAR analysis for the Chuetsu-oki earthquake discovered that the fault-related fold grew in the Nishiyama hills, which is 15 km east of the earthquake epicenter. This discovery demonstrated the advantage of InSAR for monitoring crustal deformations which exceed expectations.

Acknowledgement

The author thanks staff members of GSI for measurements of the crustal deformation related with the earthquake, helpful discussion, and encouragement. They are Mikio Tobita, Hiroshi Yarai, Shinzaburo Ozawa, Makoto Murakami (now at Hokkaido Univ.), Toru Yutsudo, Masayoshi Ishimoto, Takeshi Umesawa, Takashi Toyofuku, Satoshi Kawamoto, Tomomi Amagai, Midori Fujiwara, Akira Suzuki, Kozin Wada, Syunji Enya, Toshiyuki Sasaki, Masanori Yokokawa, Syuichi Oomori, Setsuo Tanoue, Hisao Ikeda, Moriyuki Nemoto, Hisashi Suito, Fumi Hayashi, Hiroshi Une (now at College of Land, Infrastructure, Transport and Tourism), Mamoru Koarai, and Masaharu Tsuzawa. The author is grateful to Profs. Toshihiko Kanazawa and Masanao Shinohara of the Earthquake Research Institute, University of Tokyo for providing a catalogue of precisely relocated aftershocks. The SAR data obtained using the ALOS were provided by the Japan Aerospace Exploration Agency (JAXA) through "Joint Cooperative Agreement between GSI and JAXA for observation of geographic information using Advanced Land Observing Satellite (ALOS) data."

References

Fujiwara, S., T. Nishimura, M. Murakami, H. Nakagawa, M. Tobita and P. A. Rosen (2000): 2.5-D surface deformation of M6.1 earthquake near Mt Iwate detected by SAR interferometry, Geophys. Res. Lett., 27, 2049-2052.

Geographical Survey Institute (2008): Crustal Movements in the Hokuriku and Chubu District, Rep. Coord. Comm. Earthq. Predict., 79, 403-477.

Kato, A., S. Sakai, E. Kurashimo, T. Igarashi, T. Iidaka, N. Hirata, T. Iwasaki, T. Kanazawa and Group for the aftershock observations of the 2007 Niigataken Chuetsu-oki Earthquake (2008): Imaging heterogeneous velocity structures and complex aftershock distributions in the source region of the 2007 Niigataken Chuetsu-oki Earthquake by a dense seismic observation, Earth Planets Space, 60, 1111-1116.

Koarai, M., H. Une, T. Nishimura, H. Yarai, M. Tobita and H. P. Sato (2009): Detection of surface deformation and growth of active fold induced by The Niigataken Churtsu-oki Earthquake in 2007 using SAR interferometry (in Japanese with English abstract), submitted to J. Geol. Soc. Jpn.

Kobayashi, I., M. Tateoshi, N. Yoshimura, T. Ueda and T. Kato (1995): Geological map of Japan 1:50000 “Kashiwazaki”, Geological Survey of Japan.

Nishimura, T., M. Tobita, M. Murakami, T. Kanazawa and M. Shinohara (2009): Fault Model of 2007 M = 6.8 Chuetsu-oki earthquake, central Japan, constructed using geodetic data, Advances in Geosciences (Proceedings of Asia Oceania Geosciences Society 2008), in press.

Nishimura, T., M. Tobita, H. Yarai, T. Amagai, M. Fujiwara, H. Une, and M. Koarai (2008a): Episodic growth of fault-related fold in northern Japan observed by SAR interferometry, Geophys. Res. Lett., 35, L13301, doi:10.1029/2008GL034337.

Nishimura T., M. Tobita, H. Yarai, S. Ozawa, M. Murakami, T. Yutsudo, M. Ishimoto, T. Umesawa, T. Toyofuku, S. Kawamoto, T. Amagai, M. Fujiwara, A. Suzuki, S. Enya, T. Sasaki, M. Yokokawa, S. Oomori, S. Tanoue, H. Ikeda, M. Nemoto, H. Suito, F. Hayashi, H. Une, M. Koarai and M. Tsuzawa (2008b): Crustal deformation and a preliminary fault model of the 2007 Chuetsu-oki earthquake observed by GPS, InSAR, and leveling, Earth Planets Space, 60, 1093-1098.

Ohta, Y., S. Miura, T. Iinuma, K. Tachibana, T. Matsushima, H. Takahashi, T. Sagiya, T. Ito, S. Miyazaki, R. Doke, A. Takeuchi, K. Miyao, A. Hirao, T. Maeda, T. Yamaguchi, M. Takada, M. Iwakuni, Tadafumi Ochi, Irwan Meilano and Akira Hasegawa (2008): Coseismic and postseismic deformation related to the 2007 Chuetsu-oki, Niigata Earthquake, Earth Planets Space, 60, 1081-1086.

Research Group for Active Faults of Japan (1991): Maps of Active Faults in Japan (in Japanese), University of Tokyo Press, Tokyo.

Sagiya, T., S. Miyazaki and T. Tada (2000): Continuous GPS array and present-day crustal deformation of Japan, Pure Appl. Geophys., 157, 2303-2322.

Savage, J. C. (1998): Displacement field for an edge dislocation in a layered half-space, J. Geophys. Res., 103, 2439-2446.

Shinohara, M., T. Kanazawa, T. Yamada, K. Nakahigashi, S. Sakai, R. Hino, Y. Murai, A. Yamazaki, K. Obana, Y. Ito, K. Iwakiri, R. Miura, Y. Machida, K. Mochizuki, K. Uehira, M. Tahara, A. Kuwano, S. Amamiya, S. Kodaira, T. Takanami, Y. Kaneda and T. Iwasaki (2008): Precise aftershock distribution of the 2007 Chuetsu-oki earthquake obtained by using an ocean bottom seismometer network, Earth Planets and Space, 60, 1121-1126.

Wang, R., F. L. Martin and F. Roth (2003): Computation of deformation induced by earthquakes in a multi-layered elastic crust – FORTRAN programs EDGRN/EDCMP, Computers and Geosciences, 29, 195-207.

Yamagiwa, A., Y. Hatanaka, T. Yutsudo and B. Miyahara (2006): Real-time capability of GEONET system and its application to crust monitoring, Bull. Geograph. Surv. Inst., 53, 27-33.